Kinetics and Catalysis, Vol. 44, No. 5, 2003, pp. 726–734. Translated from Kinetika i Kataliz, Vol. 44, No. 5, 2003, pp. 791–800.

CATALYTIC REACTION MECHANISMS

Mechanism of Coking on Metal Catalyst Surfaces: I. Thermodynamic Analysis of Nucleation

V. L. Kuznetsov, A. N. Usol'tseva, and Yu. V. Butenko

Boreskov Institute of Catalysis, Siberian Division, Russian Academy of Sciences, Novosibirsk, 630090 Russia

Received November 5, 2002

Abstract—Thermodynamic analysis of carbon nucleation on a metal surface is carried out. The fundamental equation is obtained that relates the critical radius of a nucleus and reaction parameters, such as temperature, metal particle oversaturation by carbon, the work of metal adhesion to graphite, and the metal–carbon bond energy. The results are compared with experimental data and conditions for the formation of carbon deposits of various kinds on metal particles are analyzed. A new mechanism for the formation of carbon nanotubes with a "bamboo" structure is proposed. This mechanism is based on a periodical change in the degree of metal particle oversaturation by carbon. The optimal conditions for the synthesis of single-wall nanotubes are formulated.

INTRODUCTION

Reactions leading to the formation of coke on the metal catalyst surfaces are very important for various catalytic processes. On the one hand, coking is the reason behind catalyst poisoning due to active surface blocking with carbon [1–4]. On the other hand, such reactions are interesting from the standpoint of obtaining carbon-containing materials with unusual carbon morphology. Specifically, such processes can be used in obtaining filamentous carbon with various structures [5–11], as well as multiple-wall and single-wall carbon nanotubes [11–14].

Due to their unique physicochemical properties, carbon nanotubes are currently a very popular subject of numerous studies into carbon compounds [11, 15, 16]. However, despite numerous papers devoted to the synthesis and properties of carbon filaments and nanotubes, the unified mechanism that combines the formation of various carbon deposits on the surfaces of metal catalysts has not been proposed. Analysis of published mechanisms for the formation of various carbonaceous materials, such as carbon filaments, multiple-wall and single-wall nanotubes, led us to conclude that they have common steps, such as the formation of a metal particle containing dissolved carbon and the formation and growth of a carbon nucleus on a metal surface. The most important of these is the step of carbon nucleus formation. Because a change in the structure of graphite-like materials (growth of structural blocks and their ordering) occurs at much higher temperatures than the temperatures of the formation of carbon particles on metal surfaces, we assumed that it is the parameters of the nucleation step that determine the critical size of a carbon nucleus and that largely stipulate the type of a graphite-like deposit. In this work we carried out the thermodynamic analysis of the step of carbon nucleation on the surface of metal particles and considered the applications of the results of this analysis for the formation of various carbon deposits. In the framework of this study we restricted ourselves to considering the processes of formation of graphite-like carbon. Note that the processes of diamond nucleation on the surfaces of various substrates have been already considered in the literature [17–19].

1. OVERVIEW OF LITERATURE MECHANISMS FOR THE FORMATION OF CARBON FILAMENTS AND TUBES

To explain the process of growth of various carbon deposits, from catalytic carbon filaments (CCF) to single-wall nanotubes, a number of mechanisms have been proposed [9, 13]. They can be divided into the following groups:

(1) The first group unites the mechanisms that involve the step of carbon dissolution in the bulk of a metal particle independently of the source of carbon (catalytic decomposition of hydrocarbons and carbon monoxide, graphite evaporation by the method of electric-arc discharge or using laser) and with further diffusion and isolation of carbon in the form of graphite-like deposits. Such a mechanism was first proposed by Baker *et al.* [20] in 1972 for the process of the formation of filamentous carbon on isolated metal particles in the catalytic decomposition of hydrocarbons. According to this mechanism, the main driving force for the formation of new carbon structures is the existence of the temperature and concentration gradients in one metal particles with carbon dissolved in it. A hydrocarbon molecule decomposes on a certain surface (plane) of a metal particle with the formation of hydrogen and carbon and with carbon dissolution in the metal bulk. The reason behind the appearance of the temperature gradient in one metal particle is local overheating of species region where hydrocarbon is decomposed. The

0023-1584/03/4405-0726$25.00

presence of the temperature gradient leads to the formation of the concentration gradient of carbon dissolved in the bulk of a metal particle. Dissolved carbon diffuses and evolves on the colder planes of a metal particle in the form of carbon fibers and filaments. Baker *et al.* [20] assumed that the diffusion of dissolved carbon is the determining step of carbon filament growth. The mechanism proposed was further improved by Buyanov *et al.* [21] who added the step of formation and decomposition of metal carbides (the carbide cycle mechanism).

It is important to note that, under conditions of synthesis of multilayer and single-layer carbon nanotubes using the methods of electric-arc discharge or laser evaporation, the reason behind carbon deposition is a decrease in the carbon solubility in metal, which is associated with a decrease in the particle temperature as it moves from the hottest zone of the arc between electrodes or from the laser evaporation zone to the zone of lower temperatures.

(2) The second group involves mechanisms that include the step of carbon diffusion along the surface a metal particle [22]. However, the diffusion of carbon along the metal surface without carbon dissolution in the metal bulk does not seem to be probable. This opinion is supported by [23] where the method of *in situ* electron microscopic imaging made it possible to observe that the interaction between the particles of iron oxide and amorphous carbon at 920 K leads to the migration of liquid-like metal particles with the formation of graphite tracks. In this case, the migration of a metal particle relative to the carbon matrix is accompanied by the dissolution of carbon.

(3) The third group involves mechanisms in which the catalyst particle only participates in the nucleation of carbon filament or tube nucleation and does not participate in the growth process [24]. According to this model, a metal particle initiates the process of formation of a primary tube consisting of graphite layers covering a metal particle. Further growth occurs via the addition of carbon atoms to the outer surface of a growing tube without metal participation. It is necessary to note that such a mechanism can probably be effective only in the presence of free atoms or small clusters of carbon in the gas phase.

(4) For the process of single-wall carbon tube formation, a mechanism was proposed according to which a cluster of several metal particles moves along the open end of the tube and continuously binds carbon atoms from the gas phase with the tube [25, 26]. However, this mechanism fails to explain the formation of ropes of single-wall nanotubes. At the same time, electron microscopic images of single-wall carbon nanotubes growing on the metal particle [27, 28] point to the formation of ropes on a single metal particle.

The thermodynamic approach to the mechanistic study of carbon nanotube growth around a spherical metal particle was used in [29]. In the model proposed, the walls of a carbon tube are nested hollow open-ended cylinders consisting of graphene planes and considered as elastodeformed planes. Tibbetts [29] considers a change in the chemical potential of the system ($\Delta\mu$) in the case of the formation of multiple-wall tubes and filaments with different outer and inner radii (r_{out} and r_{in}, respectively) as a sum of three terms: the energy of carbon surface formation (which is proportional to the free surface energy of the graphite (0002) plane), the energy of deformation (which is necessary for folding the plane graphene plate into a tube), and the chemical potential for the process of carbon atom deposition from a solution. Analysis of the dependence $\Delta\mu(r_{out}, r_{in})$ based on the condition of the maximum chemical potential $[\partial(\Delta\mu)/\partial r_{in}] = 0$ provides some optimal ratio of the inner and outer radii of the multiple-wall tube. However, this model does not consider or estimate the energy of interaction of carbon walls with a metal particle. Furthermore, the formation of open-ended graphite cylinders on a metal surface seems to be improbable since the surface energy of open ends is high (noncompensated bonds at the edges of a carbon cylinder). Note also that this model does not predict the formation of tubes with a diameter smaller than 5 nm. Therefore, this model should be refined.

Recently this model was extended to account for the case of single-wall nanotube growth [30, 31]. In these works, the process of carbon nanotube growth was considered from the standpoint of estimates of thermodynamic equilibrium between gas-phase carbon and nanotube carbon. The authors calculated the minimal diameters of nanotubes for various experimental conditions taking into account the free energies of the reactions of hydrocarbon decomposition and elasticity theory. However, they did not take into account the interaction of a growing carbon tube with the surface of a metal particle and the degree of its oversaturation with carbon.

Nevertheless, thermodynamic analysis is useful for developing the unified theory of carbon deposition on metal particles. In this work, we tried to apply thermodynamic analysis to study the step of carbon nucleation on metal. In our opinion, this step determines the form of carbon deposits on a metal surface. The determining role of the nucleation step can be supported by data on the stability of dispersed carbon fragments and carbon nuclei. This problem is especially important for the cases of multiple nuclei on the surface of a metal particle. It has been experimentally determined that ordered carbon nanostructures are sintered only at high temperatures or under the action of electron or ion beams. Thus, Kuznetsov *et al.* [32] registered the formation of mosaic structures on the diamond surface consisting of contacting multiple-wall carbon nanotubes that are stable up to 2100 K. When heating the single-wall carbon nanotubes ($d \sim 1.0$–1.5 nm) in a vacuum, argon atmosphere, or hydrogen, the process of merging of adjacent nanotubes with a doubled diameter ($d \sim 2.5$–3.0 nm) begins at 1673–1773 K [33]. With an increase in the

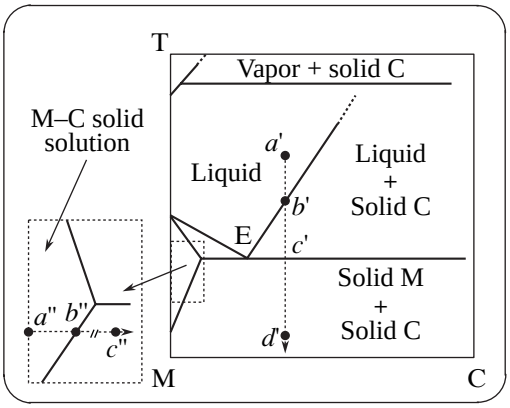

Fig. 1. Metal–carbon phase diagram (M stands for metal and C stands for carbon).

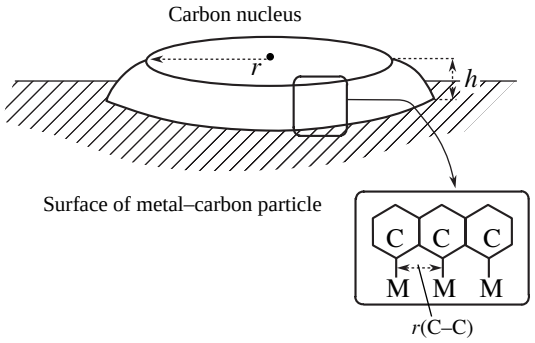

Fig. 2. Carbon nucleus on the surface of metal–carbon particle.

temperature to 2273–2673 K, the structures of carbon nanotubes change and the ordered ropes of single-wall nanotubes transform into multiple-wall tubes consisting of 2–20 carbon layers [34]. Because filamentous carbon and carbon nanotubes are formed at lower temperatures, we came to a conclusion that the nucleation step affects the type of carbon deposits formed on the metal surface.

2. ANALYSIS OF CONDITIONS FOR CARBON DEPOSITION USING THE METAL–CARBON PHASE DIAGRAM

Let us consider the generalized metal–carbon phase diagram (for metals that do not form stable carbides) in connection with the considered processes of carbon formation on a metal particle (Fig. 1). In the case of the synthesis of carbon deposits under conditions of electric-arc discharge or laser evaporation, one should consider a change in the state of a catalyst particle between points $a' \longrightarrow b' \longrightarrow c' \longrightarrow d'$. The formation of a liquid metal–carbon particle occurs in the region close to point a'. As this particle is removed from the hot zone ($a' \longrightarrow b'$) and cooled below the liquidus point (b'), carbon starts to be evolved. The equilibrium composition of the particle is determined by the liquidus line in this case. With further cooling, the particle becomes solid (the intersection of the solidus line in point c'), and carbon formation substantially slows down due to a decrease in the rate carbon diffusion through a metal particle. When cooling to lower temperatures (the region near d'), the formation of carbon discontinues. For the case under consideration, the equilibrium composition of the solid particle in the zone $c' \longrightarrow d'$ on the phase diagram is determined by the line that bounds the region of existence of the solid solution of carbon in metal. In the case of carbon deposition under the conditions of catalytic hydrocarbon or CO decomposition on solid catalysts, the pathway $a'' \longrightarrow b'' \longrightarrow c''$ is effective. In this case, the reaction temperature is much lower than in point a', and the first stage involves the process of enriching a solid metal particle with carbon and the formation of the metal–carbon solid solution (the a''–b'' region). The equilibrium concentration of carbon in this case is determined by point b''. After reaching the high degree of metal particle saturation with carbon, the process of carbon formation begins (in the region of point c'').

3. FORMATION OF CARBON NUCLEUS ON THE SURFACE OF METAL PARTICLE

3.1. Choice of the Model of a Carbon Nucleus

We consider a fragment of the graphene plane with boundary carbon atoms chemically bound to the metal surface as a primary carbon nucleus (Fig. 2). This form of nucleus is energetically preferable due to the absence of noncompensated bonds of carbon atoms. Such a structure of the carbon nucleus was proposed in [35, 36] based on the results of theoretical calculations. Such planar carbon nanostructures with a width equal to two graphene layers and a diameter of ~45 Å on a metal surface (Pd) were recently observed for the first time using the method of scanning tunneling microscopy [37]. These nuclei are planar round-shaped particles that contact the metal surface along the boundaries. In recent work [38], it was proposed that five-membered carbon rings may exist at the nucleus boundary and these rings stabilize the distorted surface of a nucleus.

3.2. Thermodynamic Analysis of Carbon Nucleation on the Metal Surface

Let us consider the formation of the planar graphite nucleus on the surface of a metal particle (Fig. 2). A change in the Gibbs energy in this case can be described as

$$\Delta G = \Delta G_{\text{nucleation}} + E_{\text{adhesion}} + E_{\text{chem.bind}} + E_{\text{def}}. \quad (1)$$

The first term ($\Delta G_{\text{nucleation}}$) is a change in the Gibbs energy in the case of isolation of $\pi r^2 h/V_M$ moles of graphite from the solution with the carbon concentration x:

$$\Delta G_{\text{nucleation}} = -\frac{\pi r^2 h}{V_M} RT \ln \frac{x}{x_0}, \quad (2)$$

where V_M is the molar volume of the graphite; R is the universal gas constant; T is the reaction temperature; h and r are the height and the radius of a nucleus; x and x_0 are the real and equilibrium concentrations of carbon in the metal–carbon solution, respectively; and x/x_0 is the degree of solution oversaturation with carbon.

The second term is a change in the free energy due to the adhesion of the carbon nucleus with the surface of a metal particle:

$$\Delta E_{\text{adhesion}} = \pi r^2(\sigma_{\text{nucl–gas}} + \sigma_{\text{nucl–surf}} - \sigma_{\text{surf–gas}}), \quad (3)$$

where σ_i are the respective surface energies. To estimate $\sigma_{\text{nucl-gas}}$ and $\sigma_{\text{surf-gas}}$, we used the value of the surface energy of graphite (basal plane) (σ_{graph}) and metal (σ_{met}), respectively. The value $\sigma_{\text{nucl-gas}}$ can be estimated using Eq. (4), which relates the surface energy of metal–graphite interaction ($\sigma_{\text{met–graph}}$) and the work of metal adhesion to the graphite surface (W_{adhesion}):

$$\sigma_{\text{met–graph}} = \sigma_{\text{graph}} + \sigma_{\text{met}} - W_{\text{adhesion}}. \quad (4)$$

Using these approximations, we can rewrite Eq. (3) in the following form:

$$\Delta E_{\text{adhesion}} = \pi r^2(2\sigma_{\text{graph}} - W_{\text{adhesion}}). \quad (5)$$

The third term estimates the energy required for the formation of a chemical bond between the boundary atoms of the carbon nucleus and the metal surface [39]:

$$\Delta E_{\text{chem.bind}} = 2\pi r\varepsilon = 2\pi r\frac{\Delta H_{\text{M–C}} - \Delta H_{\text{C–C}}}{2N_{\text{A}}r_{\text{C–C}}}, \quad (6)$$

where ε is the boundary free energy, $\Delta H_{\text{M–C}}$ and $\Delta H_{\text{C–C}}$ are the enthalpies of formation of metal–carbon and carbon–carbon bonds, respectively, $r_{\text{C–C}}$ is the distance between two nearest carbon atoms in the graphite lattice (Fig. 2), and N_{A} is the Avogadro constant. This term is necessary for the description of the nonequivalence of the carbon atom in the nucleus. A boundary atom has two bonds with a carbon atom and one bond with a metal atom, unlike other atoms of the nucleus, which have three carbon–carbon bonds each.

The fourth term estimates the deformation energy of the planar carbon nucleus, which appears due to the distortion of the graphite lattice at the boundaries when chemical bonds of the boundary atoms of a nucleus with the metal surface are formed (Fig. 2). ΔE_{def} can be estimated in the framework of the elasticity theory [39].

$$\Delta E_{\text{def}} = 2\pi r\frac{Q}{4.5h}, \quad (7)$$

where Q is a constant equal to 4.4 eV; h and r are the height and the radius of a nucleus.

Taking into account the above facts, Eq. (1) can be written in the following form:

$$\Delta G = \pi r^2\left(-\frac{h}{V_M}RT\ln\frac{x}{x_0} + (2\sigma_{\text{graph}} - W_{\text{adhesion}})\right) + 2\pi r\left(\frac{\Delta H_{\text{M–C}} - \Delta H_{\text{C–C}}}{2N_{\text{A}}r_{\text{C–C}}} + \frac{Q}{4.5h}\right). \quad (8)$$

The maximum of the function $\Delta G(r)$ corresponds to the critical size of a nucleus that can be found from the condition $d(\Delta G)/dr = 0$. Thus, we obtain the expression for the critical radius of the carbon nucleus:

$$r_{\text{cr}} = \left(\frac{\Delta H_{\text{M–C}} - \Delta H_{\text{C–C}}}{2N_{\text{A}}r_{\text{C–C}}} + \frac{Q}{4.5h}\right) \times\left[\frac{RTh}{V_M}\ln\frac{x}{x_0} + \left(W_{\text{adhesion}} - 2\sigma_{\text{graph}}\right)\right]^{-1}. \quad (9)$$

Equation (9) is the dependence of the critical radius of the carbon nucleus (r_{cr}) and the reaction parameters, such as temperature, metal particle oversaturation with carbon, and the parameters stipulated by the nature of the metal catalyst (metal–carbon bond energy and the work of metal adhesion to graphite).

3.3. Analysis of the Dependence of r_{cr} in Application to the Formation of Various Carbon Deposits

To evaluate the applicability of Eq. (9), we analyzed the dependence of the critical radius on various reaction parameters. The resulting dependence is a function of many variables: $r_{\text{cr}} = f\left(T, \Delta H_{\text{M–C}}, \frac{x}{x_0}, W_{\text{adhesion}}\right)$. In turn, these variables are not independent. Thus, the work of adhesion and the degree of oversaturation depend on temperature. Furthermore, the work of adhesion depends on the concentration of carbon in metal (that is, on the degree of oversaturation) and on the phase state of metal. For the solid state of a catalyst, it dramatically changes depending on the type of crystalline planes of a metal.

Therefore, solving Eq. (9) analytically with respect to all variables (i.e., the consideration of the effect of all reaction parameters at a time) is not possible. The graphical solution to the task under consideration is a hypersurface in the hyperspace of parameters of Eq. (9). We can only consider the corresponding cuts of this hypersurface, that is, analyze the effects of each of the reaction parameters for the constant values of the rest of parameters.

Figure 3 shows the dependence of r_{cr} on the reaction temperature calculated using Eq. (9) for iron and nickel catalysts in the solid state and melts and compares it to experimental data available in the literature. Details of calculations and the values of thermodynamic parameters were presented in [39]. When analyzing the plots of the temperature dependence of r_{cr}, it is necessary to note that at low temperatures, when carbon nuclei grow on solid metal–carbon particles, the effect of the metal nature is the most pronounced. At higher temperatures, when the metal–carbon particle is at the molten state, the effect of metal becomes less substantial. When the solid particle transforms into a liquid state, a drastic decrease in the value of the nucleus critical radius is

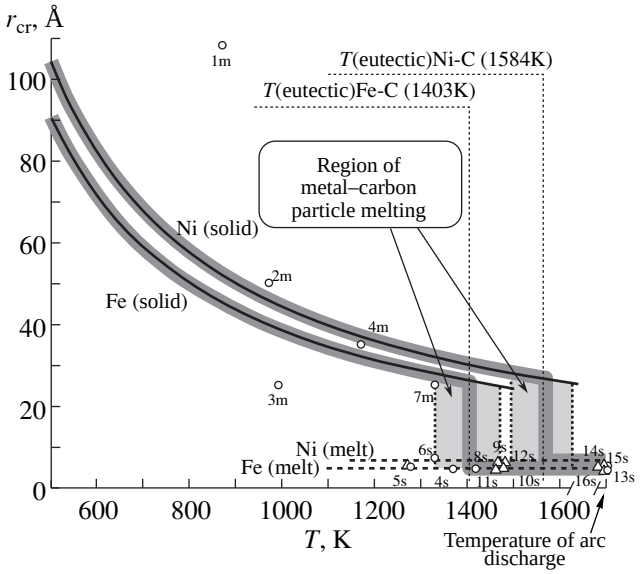

Fig. 3. Dependence of the critical radius (r_{cr}) of the carbon nucleus on the reaction temperature for Fe and Ni catalysts calculated according to Eq. (9). Open circles and triangles show and experimental data for Fe and Ni samples, respectively. Each experimental point is labeled by the literature reference and a letter (m for multiple-wall and s for single-wall carbon nanotubes).

observed. A substantial difference in the critical radii of nuclei for the solid and molten states of the catalyst is due to a considerable difference in the work of adhesion for these metal states. The process of metal–carbon particle melting occurs at temperatures close to the temperature of metal–carbon eutectics. However, a decrease in the melting point is possible due to decrease in the size of metal particles or due to the presence of admixtures of other elements (S, P, Sb, etc.).

Note that r_{cr} for the carbon nucleus that we try to estimate is the lower limit for the radius of carbon deposits. Nuclei with a radius lower than critical are unstable and will dissolve in the bulk of metal particles. Nuclei with a larger radius may continue to grow and the radii of tubes or fibers may be larger than the critical value. Thus, the critical size of a nucleus determined the lower value for the radius of carbon deposits formed under certain conditions. When estimating r_{cr} for solid particles, the situation is complicated by the lack of data on the value of work of adhesion to graphite for various metals and solid metal–carbon solutions. We had to use the average value of the work of adhesion for solid metals (0.024 cal/m^2). These facts explain the disagreement of estimates and experimental data for the solid state of metal catalyst particles. At the same time, almost all points obtained from the analysis of experimental data for multiple-wall carbon nanotubes and filamentous carbon agree with the calculations that made use of Eq. (9). The minimal apparent sizes of internal channels of carbon tubes and the cross-sections of carbon are larger than those calculated for the critical nucleus.

Figure 4 also shows the dependence of r_{cr} on other thermodynamic parameters, such as the degree of oversaturation of a metal–carbon particle with carbon (x/x_0), the enthalpy of formation of a metal–carbon bond (ΔH_{M-C}), the work of adhesion of metal to graphite ($W_{adhesion}$), and the surface free energy of graphite (σ_{graph}). Calculations were carried out for the iron catalyst in the solid and molten states (for temperatures of 773 and 1473 K, respectively). It can be seen from the plots that the critical sizes of a nucleus are most sensitive to changes the degree of oversaturation and the work of adhesion (Figs. 4a, 4d). The degree of oversaturation affects both a change in the value of the ratio x/x_0 in Eq. (9) and the work of adhesion ($W_{adhesion}$). Thus, it was found in [40] that $W_{adhesion}$ for molten metal particles changes depending on the concentration of carbon in a melt. In our estimates, we used the value of the work of adhesion for the concentration of carbon in metal that is close to the eutectic state of the corresponding metal–carbon system.

Thus, the reaction temperature, the degree of metal particle oversaturation with carbon $\left(\frac{x}{x_0}\right)$, and the work of adhesion have the most pronounced effect on the critical radius of a nucleus of all the reaction parameters studied.

3.4. Choice of Optimal Conditions for Single-Wall Carbon Nanotubes

Analysis carried out in this work allowed us to formulate optimal conditions for the purposeful synthesis of single-wall carbon nanotubes:

(1) An increase in the reaction temperature leads to the formation of nuclei with smaller radii and, in the limiting case, to the growth of single-wall nanotubes.

(2) The nucleation and growth of single-wall nanotubes mostly occurs on liquid metal particles.

(3) For the synthesis of single-wall nanotubes on solid catalyst particles, the high degree of metal particle oversaturation is demanded.

(4) Other conditions being the same, the use of catalysts with a high value of the metal–carbon bond energy leads to the formation of nanotubes with smaller diameters.

Thus, the optimal reaction pathway for the synthesis of single-wall nanotubes corresponds to the line $a' \longrightarrow b' \longrightarrow c' \longrightarrow d'$ on the metal–carbon phase diagram (Fig. 1). In this case, carbon nucleation occurs on the liquid metal particle when the reaction temperature will reach a value lower than point b'. These conditions can usually be realized using the methods of electric arc discharge and laser evaporation. Single-wall nanotube synthesis is a also possible under isothermic conditions of the catalytic decomposition of hydrocarbons or CO

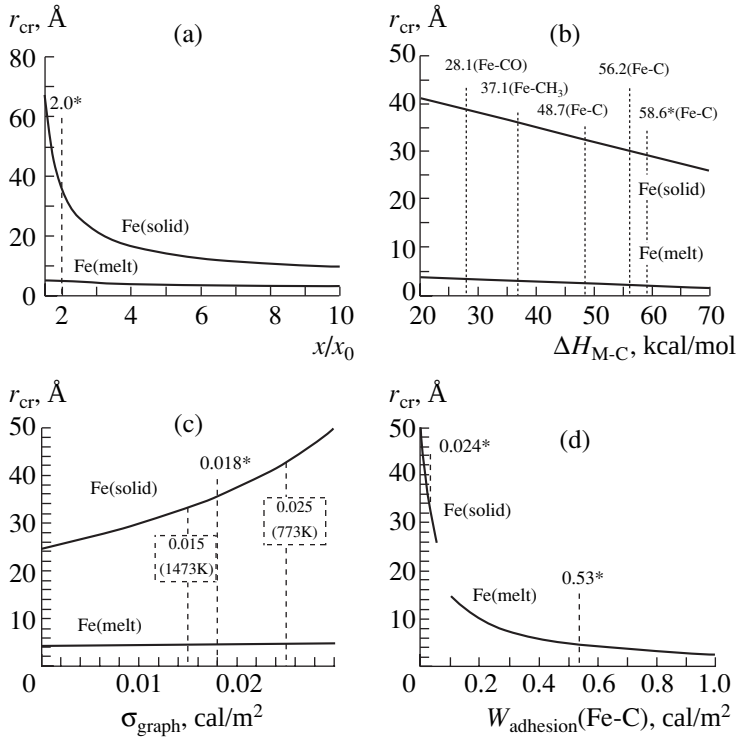

Fig. 4. Dependence of the critical radius (r_{cr}) of the carbon nucleus on (a) the degree of oversaturation of the metal–carbon particle by carbon, (b) the enthalpy of formation of a metal–carbon bond, (c) surface energy of graphite, and (d) the work of adhesion of iron to graphite. (The star marks the values used in our estimates.)

on solid metal particles (the line $a'' \longrightarrow b'' \longrightarrow c''$) if the high degree of metal particle oversaturation with carbon is reached (point c''). The use of highly dispersed metal catalysts can be favorable for reaching the high degrees of oversaturation.

4. VARIOUS SCENARIOS OF NUCLEUS FORMATION AND GROWTH

A nucleus with a radius lower than critical is unstable and can be dissolved in the bulk of a metal particle. Obviously, the critical size of a nucleus is dependent on the nature of a metal and on the specific conditions of the reaction. Let us consider the effect of the critical size of the nucleus on the morphology of the graphite-like deposits.

4.1. The Formation of Capsulated Metal Particles and Catalytic Filamentous Carbon

When the critical size of a nucleus is high ($r_{cr} \geq 10$–20 nm), one may expect the formation of prolonged carbon layers that lead to the appearance of metal particles or to the formation of carbon filaments characterized by the large area of contact between the metal particle and the graphene plane. Depending on the preferable orientation of graphene planes relative to the axis of a growing filament, carbon filaments may have a coaxial–cylindrical or a coaxial–conical structure [41], which is also called "fish skeleton." In addition to that, a structure may be observed in which graphene planes are oriented relative to the metal surface as a pack of cards.

4.2. The Formation of Single-Wall Nanotube Ropes

In the formation of small ($r \sim 0.35$–1.5 nm) multiple nuclei, single-wall carbon nanotubes is probable. The interaction of nuclei with each other may result in the formation of close-packed mosaic structures on the surface. A further growth of such structures leads to the formation of ropes of close-packed single-wall nanotubes.

4.3. The Formation of Multiple-Wall and Bamboo-like Carbon Nanotubes

When the size of a critical nucleus is intermediate, the formation of more or less ordered coaxial-cylindrical structures is typical, which are multiple-wall carbon nanotubes. The outer diameter of a multiple-wall tube usually corresponds to the diameter of a metal particle on which it grows. The inner diameter of a multiple-wall tube cannot be smaller than the critical size of a carbon nucleus. In this case, tubes of two types can be formed: with and without internal partition.

The formation of multiple-wall tubes or filaments with internal partitions was observed by many

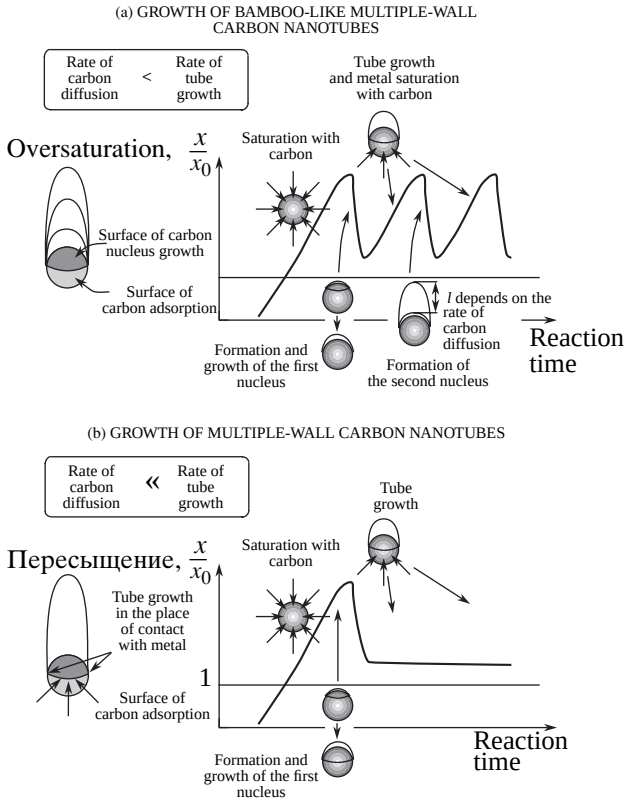

Fig. 5. The scheme of growth of various multiple-wall carbon nanotubes.

researchers [42, 43]. Such tubes were called bamboo-like because of their structures. Saito [44] proposed a mechanism for the growth of such tubes in electric-arc discharge in the presence of nickel. According to this mechanism, the formation of carbon in the form of graphite-like concentric layers occurs on the surface of a metal particle with periodical supplanting of a metal particle due to poor wetting of a graphite surface (the internal channel of a growing tube) by metal. Kovalevski and Safronov [45] proposed a mechanism for the growth of bamboo-like tubes in the course of hydrocarbon pyrolysis in the presence of metals. According the model proposed in [45], capsulated metal particles are formed in the course of synthesis. An increase in the temperature leads to the widening of a metal particle and to the rupture of the carbon coating with pushing a metal particle out. According to the authors, altered capsulation and pushing a metal particle out of the carbon coating leads to the formation of a "bamboo-like structure." Unfortunately, the authors did not mention possible reasons for the periodical heating of the metal particle. Wang *et al*. [46] recently observed the formation of bamboo-like tubes in the thermal decomposition of iron phthalocyanine. They assumed that the formation of such tubes is due to sliding a carbon fragment, which tightly envelopes a metal particle from the one side due to the accumulation of tension with an increase in the sizes of such fragments. An analogous scheme of the growth was proposed in [47]. However, none of the cited mechanisms provides adequate explanation for the processes leading to the supplanting of a metal particle or to the sliding of a carbon fragment.

Let us consider the formation of bamboo-like tubes using the results of thermodynamic analysis carried out in this work. Analysis of Eq. (9), which characterizes the dependence of the critical radius of a nuclei on experimental parameters, provides explanation for the formation of bamboo-like tubes from the standpoint of cyclic changes in the degree of oversaturation of metal catalyst particle by carbon right in the region of its contact with a growing carbon tube. It is known that the rate-limiting step in the growth of carbon tubes is carbon diffusion through the metal particle. This is confirmed by experiments on changes in the growth rate of carbon filaments [48]. Specifically, it was found that the rate is inversely proportional to the diameter of filaments at the initial stage of the growth process [49, 50]. Therefore, we may assume that, after the formation of a critical carbon nucleus on the surface, the primary nucleus grows under which new nuclei are continuously formed and grow. This results in the formation of several graphene layers. Because of the low rate of carbon atom diffusion, its concentration in the near-surface layer of the metal (and, correspondingly, the degree of oversaturation) drastically decreases. Such a situation can take place under nonstationary conditions when a flow of carbon diffusing inside a metal particle is less intensive than a flow of carbon consumed for the growth of a tube (Fig. 5a). Because each value of the degree of oversaturation corresponds to a certain critical radius of a nucleus (Fig. 4a), such a decrease in the degree of oversaturation leads to an increase in the value of the critical radius for the next nucleus. The formation of a new nucleus with a radius larger than the inner radius of a tube channel is impossible. Under these conditions, the insertion of carbon atoms into metal–carbon bonds would occur at the edges of a growing nucleus and lead to the growth of a hollow tube. Tube elongation will continue until oversaturation with carbon in the near-surface layer would reach a value sufficient for the formation of a new nucleus with a critical radius that is lower than or equal to the size of the inner channel of a tube. After the growth of this nucleus, which partition a growing tube, the concentration of carbon in the near-surface layer will decrease, the tube will grow, and the particle will saturate with carbon until its concentration will be sufficient for the appearance of a nucleus with the critical radius smaller than or equal to the inner size of a tube. Thus, the most probable reason for the formation of bamboo-like tubes is the periodical change in the degree of metal particle oversaturation by carbon.

If the degree of oversaturation by carbon in the near-surface layer of the metal particle under the primary nucleus is not sufficient for the appearance of the critical nucleus, hollow multiple-wall nanotubes are not formed (Fig. 5b).

CONCLUSIONS

Thermodynamic analysis of the step of carbon nucleation on the metal surface has been carried out. The dependence of the critical radius of the carbon nucleus on the reaction parameters, such as temperature, metal particle oversaturation by carbon, the metal–carbon bond energy, and the work of adhesion of metal to graphite has been obtained. Conditions for the formation of various carbon deposits on metal particles have been analyzed. Optimal conditions for the synthesis of single-wall carbon nanotubes have been formulated. Based on the dependence of the critical radius of the carbon nucleus, a mechanism has been proposed for the formation of bamboo-like tubes.

ACKNOWLEDGMENTS

This work was supported by the Russian Foundation for Basic Research (grant no. 02-03-32296), INTAS (00-237), YSF (2001/2-109), and CRDF (REC 008).

REFERENCES

1. Buyanov, R.A., *Zakoksovanie katalizatorov* (Catalyst Coking), Novosibirsk: Nauka, 1983.
2. Rostrup-Nielsen, J.R., *J. Catal.*, 1984, vol. 85, p. 31.
3. Hughes, R., *Dezaktivatsiya katalizatorov* (Catalyst Deactivation), Moscow: Khimiya, 1983, p. 280.
4. *Deactivation and Poisoning of Catalysts*, New York: Var. Dekker, 1985, p. 327.
5. Trimm, D.L., *Catal. Rev. – Sci. Eng.*, 1977, vol. 16, p. 155.
6. Rostrup-Nielsen, J.R. and Trimm, D.L., *J. Catal.*, 1977, vol. 48, p. 155.
7. Baker, R., *T.K. Carbon Fibers, Filaments, and Composites*, Figueiredo, J.L., Ed., Dordrecht: Kluwer, 1990, p. 405.
8. Rodriguez, N., *J. Mater. Res.*, 1993, vol. 8, p. 3233.
9. Dresselhaus, M.S., Dresselhaus, G., Sugihara, K., Spain, I.L., and Goldberg, H.A., *Graphite Fibers and Filaments*, Berlin: Springer, 1988, p. 20.
10. De Jong, K.P. and Geus, J.W., *Catal. Rev. – Sci. Eng.*, 2000, vol. 42, no. 4, p. 481.
11. *Carbon Filaments and Nanotubes: Common Origins, Differing Applications?*, Biro, L.P., Bernardo, C.A., Tibbets, G.G., and Lambin, Ph., Eds., Dordrecht: Kluwer Academic, 2001, vol. 372.
12. Iijima, S., *Nature*, 1991, vol. 354, p. 56.
13. Endo, M., Saito, R., Dresselhaus, M.S., and Dresselhaus, G., *Carbon Nanotubes: Preparation and Properties*, Boca Raton: CRC, 1997, p. 54.
14. Ajayan, P., *Chem. Rev.*, 1999, vol. 99, p. 1787.
15. Ebbesen, W.T., *Carbon Nanotubes: Preparation and Properties*, Boca Raton: CRC, 1997, p. 225.
16. Eletskii, A.V., *Usp. Fiz. Nauk*, 1997, vol. 167, no. 9, p. 945.
17. Deryagin, B.M. and Fedoseev, D.V., *Usp. Khim.*, 1970, vol. 39, no. 9, p. 1661.
18. Wong, M.-S., Lu, C.-A., Chang, H.-K., Yang, T.S., Wu, J.-H., and Liou, Y., *Thin Solid Films*, 2000, vols. 377–378, p. 274.
19. Lux, B. and Haubner, R., *Diamond and Diamond-like Films and Coating*, Clausing, R.E., Ed., New York: Plenum, 1991.
20. Baker, R.T.K., Barber, M.A., Harris, P.S., Feates, F.S., and Waite, R.J., *J. Catal.*, 1972, vol. 26, p. 51.
21. Buyanov, R.A., Afanas'ev, A.D., and Chesnokov, V.V., *Kinet. Katal.*, 1979, vol. 20, p. 207.
22. Oberlin, A., Endo, M., and Koyama, T., *Carbon*, 1976, vol. 14, p. 133.
23. Krivoruchko, O.P., Zaikovskii, V.I., and Zamaraev, K.I., *Dokl. Akad. Nauk*, 1993, vol. 329, p. 744.
24. Gamaly, E.G., *Carbon Nanotubes: Preparation and Properties*, Ebbesen, T.W., Ed., Boca Raton: CRC, 1997, p. 180.
25. Thess, A., Lee, R., Nikolaev, P., Dai, H., Petit, P., Robert, J., Xu, C., Lee, Y.H., Kim, S.G., Rinzler, A.G., Colbert, D.T., Scuseria, G.E., Tomanek, D., Fischer, J.E., and Smalley, R.E., *Science*, 1996, vol. 273, p. 483.
26. Kiang, C.-H. and Goddard III, W.A., *Phys. Rev. Lett.*, 1996, vol. 76, p. 2515.
27. Kataura, H., Kimura, A., Ohtsuka, Y., Suzuki, S., Maniwa, Y., Hanyu, T., and Achiba, Y., *Jpn. J. Appl. Phys.*, 1998, vol. 37, p. 616.
28. Zakharov, D.N., *Cand. Sci. (Phys.–Math.) Dissertation*, Moscow: Inst. of Crystallography, 2001.
29. Tibbetts, G.G., *J. Cryst. Growth*, 1984, vol. 66, p. 632.
30. Kanzow, H. and Ding, A., *Phys. Rev. B*, 1999, vol. 60, no. 15, p. 11180.
31. Kanzow, H., Bernier, P., and Ding, A., *Appl. Phys. A*, 2002, vol. 74, p. 411.
32. Kuznetsov, V.L., Chuvilin, A.L., Butenko, Y.V., Stankus, S.V., Khairulin, R.A., and Gutakovskii, A.K., *Chem. Phys. Lett.*, 1998, vol. 289, p. 353.
33. Nikolaev, P.N., Thess, A., Rinzler, A.G., Colbert, D.T., and Smalley, R.E., *Chem. Phys. Lett.*, 1997, vol. 266, nos. 5–6, p. 422.
34. Bougrine, A., Dupont-Pavlovsky, N., Naji, A., Ghanbaja, J., Mareche, J.F., and Billaud, D., *Carbon*, 2001, vol. 39, p. 685.
35. Tontegode, A.Ya. and Rut'kov, E.V., *Fiz. Tverd. Tela*, 1987, vol. 29, p. 1306.
36. Tontegode, A.Ya., *Poverkhnost.*, 1988, vol. 8, p. 13.
37. Dulot, F., Eugene, J., Kierren, B., Malterre, D., and Eltsov, K.N., *Phys. Low-Dim. Struct.*, 1999, vols. 1/2, p. 217.
38. Gavillet, J., Loiseau, A., Journet, C., Willaime, F., Ducastelle, F., and Charlier, J.-C., *Phys. Rev. Lett.*, 2001, vol. 87, no. 27, p. 275504.
39. Kuznetsov, V.L., Usoltseva, A.N., Chuvilin, A.L., Obraztsova, E.D., and Bonard, J.-M., *Phys. Rev. B*, 2001, vol. 64, p. 235401.
40. Naidich, Yu.V., Perevertailo, V.M., Lavrinenko, I.A., Kolisnichenko, G.A., and Zhuravlev, V.S., *Poverkhnostnye svoistva rasplavov i tverdykh tel i ikh ispol'zovanie v materialovedinii* (Surface Properties of Melts and Solids and Their Use in Material Science), Naidicha, Yu.V., Ed., Kiev: Naukova Dumka, 1991, p. 64.

41. Rodriguez, N.M., Chambers, A., and Baker, R.T.K., *Langmuir*, 1995, vol. 11, p. 3862.
42. Endo, M., *J. Phys. Chem. Solids*, 1993, vol. 54, no. 12, p. 1841.
43. Saito, Y., *J. Phys. Chem. Solids*, 1993, vol. 54, no. 12, p. 1849.
44. Saito, Y., *Carbon*, 1995, vol. 33, no. 7, p. 979.
45. Kovalevski, V.V. and Safronov, A.N., *Carbon*, 1998, vol. 36, nos. 7–8, p. 963.
46. Wang, X., Hu, W., Liu, Y., Long, C., Xu, Y., Zhou, S., Zhu, D., and Dai, L., *Carbon*, 2001, vol. 39, p. 1533.
47. Blank, V.D., Gorlova, I.G., Hutchison, J.L., Kiselev, N.A., Ormont, A.B., Polyakov, E.V., Sloan, J., Zakharov, D.N., and Zybtsev, S.G., *Carbon*, 2000, vol. 38, p. 1217.
48. Baker, R.T.K., Chludzinski, J.J., and Lund, C.R.F., *Extended Abstracts of the 18th Biennial Conference on Carbon*, Worcester Polytechnic Institute: American Carbon Society, 1987, p. 155.
49. Endo, M. and Komaki, K., *Extended Abstracts, of the 16th Biennial Conference on Carbon*, San Diego, CA, American Carbon Society, University Park, PA, 1983, p. 523.
50. Tibbetts, G.G., Devour, M.G., and Rodda, E.J., *Carbon*, 1987, vol. 25, p. 367.

APPENDIX

Reference for Fig. 3.

1. Downs, W.B. and Baker, R.T.K. *J. Mater. Res.*, 1995, vol. 10, p. 625.
2. Ivanov, V., Nagy, J.B., Lambin, Ph., Lucas, A., Zhang, X.B., and Zhang, X.F., Bernaerts, D., van Tendeloo, G., Amelinckx, S., and van Landuyt J., *Chem. Phys. Let.*, 1994, vol. 223, p. 329.
3. Hernadi, K., Fonseca, A., Nagy, J.B., Bernaerts, D., and Lucas, A.A., *Carbon*, 1996, vol. 34, p. 1249.
4. Bladh, K., Folk, L.K.L., and Rohmund, F., *Appl. Phys. A*, 2000, vol. 70, p. 317.
5. Bandow, S., Asaka, S., Saito, Y., Rao, A.M., Grigorian, L., Richter, E., and Eklund, P.C., *Phys. Rev. Let.*, 1998, vol. 80, p. 3779.
6. Peigney, A., Laurent, Ch., Dobigeon, F., and Rousset, A., *J. Mater. Res.*, 1997, vol. 12, p. 613.
7. Cheng, H.M., Li, F., Sun, X., Brown, S.D.M., Pimenta, M.A., Marucci, A., Dresselhaus, G., and Dresselhaus, M.S., *Chem. Phys. Lett.*, 1998, vol. 289, p. 602.
8. Thess, A., Lee, R., Nikolaev, P., Dai, H., Petit, P., Robert, J., Xu, C., Lee, Y.H., Kim, S.G., Rinzler, A.G., Colbert, D.T., Scuseria, G.E., Tomanek, D., Fischer, J.E., and Smalley, R.E., *Science*, 1996, vol. 273, p. 483.
9. Dai, H., Rinzler, A.G., Nikolaev, P., Thess, A., Colbert, D.T., and Smalley, R.E., *Chem. Phys. Lett.*, 1996, vol. 260, p. 471.
10. Yudasaka, M., Yamada, R., Sensui, N., Wilkins, T., Ichihashi, T., and Iijima, S., *J. Phys. Chem. B.*, 1999, vol. 103, p. 6224.
11. Qin, L.-C. and Iijima, S., *Chem. Phys. Let.*, 1997, vol. 269, p. 65.
12. Takahashi, H., Sugano, M., Kasuya, A., Saito, Y., Kayama, T., and Nishina, Y., *J. Mater. Sci. Eng. A: Struct. Mater.*, 1996, vol. 217, p. 48.
13. Saito, Y., Okuda, M., Fujimoto, N., Yoshikawa, T., Tomita, M., and Hayashi, T., *Jpn. J. Appl. Phys.*, 1994, vol. 33, p. L526.
14. Williams, K.A., Tachibana, M., Allen, J.L., Grigorian, L., Cheng, S-C., Fang, S.L., Sumanasekera, G.U., Loper, A.L., Williams, J.H., and Eklund, P.C., *Chem. Phys. Lett.*, 1999, vol. 310, p. 31.
15. Saito, Y., Koyama, T., and Kawabata, K., *Z. Phys. D*, 1997, vol. 40, p. 421.